Published by :
http://www.ijert.org

International Journal of Engineering Research & Technology (IJERT)
ISSN: 2278-0181
Vol. 11 Issue 10, October-2022

Development of A Fully Faired Recumbent Bike using A Three-Piece Mold

Hrishabh Jha[1], Avhishek Jha[1], Kunal Nath[1], Rajesh Kumar[2]
[1] Department of Mechanical Engineering, Delhi Technological University, Delhi
[2] Professor, Department of Mechanical Engineering, Delhi Technological University, Delhi, India

***Abstract*—Sustainable transportation is the ability to meet the mobility needs of a society without causing any damage to the environment and impairing the mobility needs of future generations. It comprises low and zero-emission, energy-efficient, affordable modes of transport, including electric and alternative-fuel vehicles. The project aims to create a fully faired recumbent to combat the energy crisis by providing a sustainable alternative to regular commuters over other conventional means of transportation. The primary goal is to develop an adaptable, technically feasible and economically successful HPV. The frame material of the bike is made of Chromoly Steel core, and it includes an adjustable Bottom Bracket Clamp to allow riders of different heights to ride comfortably. The flexibility to accommodate various riders makes the recumbent bike suitable as a commuter vehicle. The fairing is designed on SolidWorks and fabricated with Carbon Fiber using a 3-piece mold. Adherence to essential safety standards is assured through Roll-over Protection System Analysis, Structural Analysis, and Aerodynamic Analysis on ANSYS.**

Keywords—Sustainable Transportation; Recumbent; Velomobile; SolidWorks; ANSYS; Carbon Fiber; Roll-over Protection System

I. INTRODUCTION

Recumbents are human-powered vehicles, further enclosed with a fairing (aerodynamic shell) for improving aerodynamic performance and protection from weather and collisions. Any streamlined human powered vehicle consisting of a full fairing could be referred to as a velomobile [1,2].

The design goal of the vehicle was to create a state-of-the-art human powered vehicle, which can handle real life situations, enhancing vehicle safety and practicality, particularly as a form of everyday transportation and be a safer, fast, and lightweight vehicle. Diversification of recumbent geometries were studied as per the American Society of Mechanical Engineers (ASME) guidelines along with different types of bicycles and trikes, which helped determine a fully faired, low racer bike as the most suitable option to achieve the defined project goals.

The design/processes that were developed/adopted and used for vehicle:
a. Use of wooden jigs to determine the constraints upon which the frame and fairing were developed.
b. Use of blue foam for the box ribbing of the fairing.
c. Number of layers of carbon fiber to be used is decided upon the strength testing done in the previous year.
d. 3-piece mold technique was used.

The ASME HPVC 2019 constraints [3] were used and any measure to increase rider, team members and bystander's safety without compromising the performance, stability and ride quality of the vehicle guided Vehicle's Design.

TABLE 1. DESIGN SPECIFICATIONS FROM ASME CONSTRAINTS

	ASME Constraints	Project Goals
Safety	• Have a Roll-over Protection System (RPS) that will: ○ Produce less than 5.1 cm of total deformation of application of 2670 N of top load (At an angle 12° away from the front) ○ Produce less than 3.8 cm of total deformation of application of 1330 N side load. ○ No body contact and adequate abrasion resistance in the event of a fall and slide respectively. • Include safety harness that holds rider to vehicle during a crash • Include Head/Tail light, bell or horn, front/rear/side reflectors • Field of View of at least 180° • Free from sharp edges, open tubes, protruding screws or any other potential hazards	• The RPS at all points has a reasonable FOS (> 2.5) at all points and the von – misses stress is below the maximum tensile strength. • The safety attachment points stay intact in the event of emergency stop. • The steering system remains intact in the event of a crash • The horn is easily accessible. • No exposed wires and all batteries are located away from the rider. • Use commercially available seat harness
Performance	• Demonstrate stability at 5-8 km/hr for 30m (fast paced walking speed). • Brake from 25 to 0 km/hr in 6 m • Turn within an 8 m radius (26.2 ft) • Clear a speed bump with maximum height up to 5 cm. • Transport a parcel with dimensions 38x33x20 cm and a maximum mass of 5.5 kg.	• Total Weight less than 25kg • Top Speed of 90 kmph • Easy rider Ingress/Egress using Better Rider Comfort • Minimize the overall drag experienced by the fairing • Create a more efficient drivetrain for achieving higher top speed. • Maximum vehicle length less than 8.5 ft (2.6 m)
Rider	• Log a minimum of 30 minutes of vehicle riding experience before the event. • The rider must wear appropriate clothing and properly fitting helmets with fastened straps that CPSC Safety Standard for Bicycle Helmet (16 CFR Part 1203)	• Attend three workouts per weeks focused on improving stamina, strength and overall fitness. • Cycling sessions which simulate actual competition three times a week

II. METHOD

A House of Quality was done to determine factors to focus on. Drivetrain efficiency and Rider satisfaction were identified as the primary factors over other factors. This is decided based on the importance rating given to the metrics analogous to the project requirements. The other factors, which were of high priority, consisted of Field of view, ergonomics, and vehicle weight [4].

Product Design Specifications obtained for designing the vehicle obtained from the HOQ and ASME constraints are as follows. Based on the design criteria and Quality Function Deployment, the Pugh's concept selection technique is adopted [5].

International Journal of Engineering Research & Technology (IJERT)
ISSN: 2278-0181
Vol. 11 Issue 10, October-2022

Product Design Specifications obtained for designing the vehicle obtained from the HOQ and ASME constraints are as follows. Based on the design criteria and Quality Function Deployment, the Pugh's concept selection technique is adopted [5].

TABLE 2. PRODUCT DESIGN SPECIFICATIONS

Metric	Target Value
Coefficient of Drag	< 0.1
Field of View	225°
Turning Radius	< 5 m
Rider Satisfaction	9/10
Weight	30 kg
Cost	< INR 200,000
Rider Height Range	20 cm
Braking distance from 25 kmph speed	< 6 m
Low Speed Stability	Stable at 5 kmph for 30m

TABLE 3. RATING CRITERIA

Score	Quality
5	Excellent
4	Good
3	Average
2	Poor
1	Very Poor

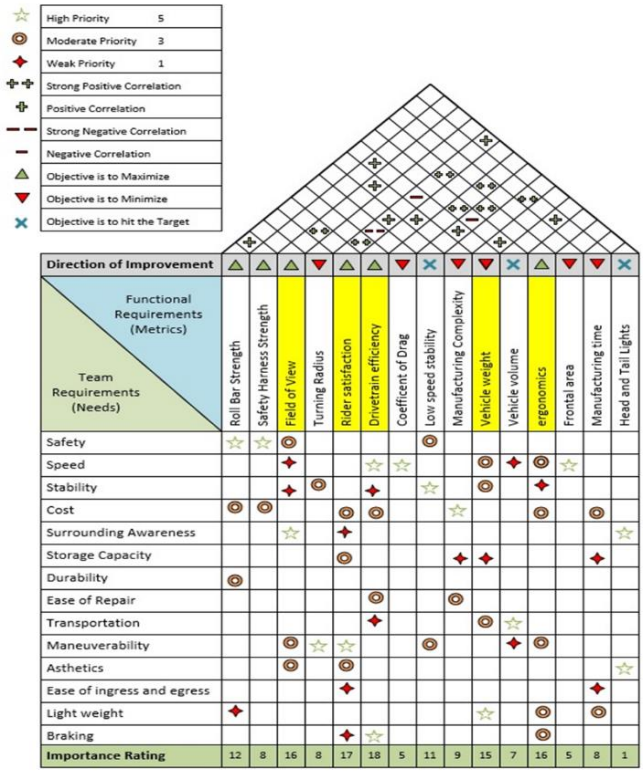

Fig. 1. House of Quality

A decision matrix was made with weighted average given to each category for critical design considerations.

TABLE 4. DECISION MATRIX FOR VEHICLE TYPE

Metric	Weightage (%)	Fully faired recumbent low racer	Partially Faired Low Racer	Trike	Upright Partially Faired	Tadpole (Recumbent)
Frame weight	14	4	3	3	5	2
Aerodynamics	17	5	4	3	1	3
Rider Comfort	15	4	4	4	3	4
Speed	15	5	4	3	2	2
Maneuverability	12	3	4	4	5	3
Prior Knowledge	13	5	4	3	5	2
Drivetrain Efficiency	14	4	3	3	5	3
Total	100	4.33	3.72	3.27	3.57	2.73

The vehicle configuration was decided after considered various possibilities for vehicle geometries and determining a score based on QFD corresponding to each category. A fully faired recumbent low racer configuration is concluded as the most effective based on all the above metrics.

A similar comparative study was done for the frame body using a variety of materials namely AISI 4130 Chromoly Steel, AISI 1020 Steel, Aluminium 6061, and Carbon Fiber. AISI 4130 Chromoly Steel was selected based on the decision matrix. The difference between total metric value of AISI 4130 and Carbon Fiber is insignificant; however, due to easy machining AISI 4130 Chromoly Steel is preferred.

TABLE 5. DECISION MATRIX FOR FRAME MATERIAL

Metric	Weightage (%)	Aluminum 6061	AISI 1020 Steel	AISI 4130 Chromoly Steel	Carbon Fiber
Strength/ Weight Ratio	18	4	1	4	5
Ease of Machining	21	3	4	4	3
Ease of Repair	12	3	4	4	3
Availability	9	4	5	3	3
Cost	7	3	5	3	2
Durability	11	3	4	4	3
Weight	13	4	1	4	5
Corrosion Resistance	4	4	3	4	5
Recyclability	5	4	4	3	3
Total	100	3.49	3.13	3.79	3.63

FWD has several advantages over RWD primarily shorter and more efficient drivetrain, lesser vibrations, lesser no. of idlers, compact drivetrain [6]. Although the major issue of "Heel Strike" is present in FWD, still it was considered because of other benefits. The issue of heel strike was tackled by changing the Bottom-bracket height and avoiding the use of derailleur hanger. The multichain drivetrain results in more gear ratio choices, but derailment and complexity of the drivetrain increases. Thus, a single chain drivetrain was selected.

The seat height was kept at 28 cm and seat back angle at 40 degrees to increase rider comfort. The seatback and headrest angles were decided based on rider inputs.

TABLE 6. DECISION MATRIX FOR DRIVETRAIN

Criteria	Weightage (%)	Single Chain	Multi Chain
Efficiency	40	5	3
Gear Reduction	30	1	2
Manufacturability	20	4	3
Cost	10	4	3
Total	100	3.5	2.7

TABLE 7. FRAME PARAMETERS

Parameter	Value
Front Wheel Diameter	0.497 m
Head Tube Angle	73.4°
Wheel Base	1.24 m
Trail	0.55 cm

The vehicle was designed on a Front Wheel Drive comprising of a single 60 teeth chainring and Shimano 8 speed cassette shifting mechanism [7,8]. A threaded Bottom bracket mechanism with an aluminium spider crank with crank arm length 165 mm was installed on the frame. Two idlers were used for proper routing and idler sizing was done to provide tension relief to the second idler which was directly routed to

International Journal of Engineering Research & Technology (IJERT)
ISSN: 2278-0181
Vol. 11 Issue 10, October-2022

the derailleur. The drivetrain was selected as per market availability. Idler dimensions were optimized to prevent chain derailment.

Fig. 2. Recumbent bike frame

A fairing provides the added advantage of protecting the rider from dust, dirt, and other unwanted obstacles. High emphasis was given on the aerodynamic stability of the vehicle. The designing process involved using a Java Applet named JavaFoil, on which NPL ECH and NACA 6 series were considered for the sections of the vehicle [9,10]. The ECH 2866 met the needs of the team dimensionally for the top section of the fairing and ECH 4466 for the side section. These sections were further modified to achieve close to ideal fairing design.

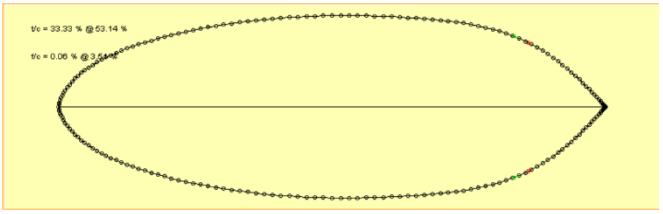

Fig. 3. ECH 2866 NACA 6 series design

A fully faired carbon fiber fairing using two female molds of glass fiber was made in which carbon fiber was laid up. The upper mold was then divided into two parts for partition of door and to reduce the seam length which led to a three-piece mold structure. This reduced the number of cuts for the door from four to one. CBF (car body filler) was used at places with severe depressions and the molds were sanded with different grit sizes of sandpaper ranging from 240 to 1200 to get the perfect surface finish to the molds for Carbon Fiber Layup. The fairing of vehicle was made from Carbon Fiber using vacuum bagging and conventional hand layup techniques.

Fig. 4. Fairing Mold

Fig. 5. Partition for door

Rib placement was given a special emphasis to form a structural member throughout the vehicle [11]. Ribs made of blue foam were strategically placed along the regions which must be cut such as the front wheel and windshield and along the RPS, where the rider's movement is not obstructed, and where the rider is to be seated. The fairing's removable top hatch was mainly for the ingress/egress of the rider. Even after removal of the top hatch, the rider was protected by the fairing RPS in the event of a crash. The rear hatch houses the rear braking, electronics components, and storage area.

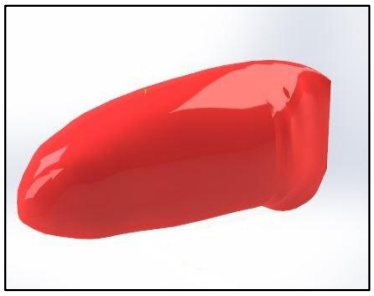

Fig. 6. Fairing CAD Design

III. ANALYSIS

A. Roll-over Protection System Analysis

Considering the safety of the rider to be of utmost priority, the vehicle incorporates a strategically designed roll bar to prevent the rider from direct contact with the road surface and to reduce the impact of any accidental collision. A four-point seat belt was used with attachment points to the side rod and the bottom of the RPS was chosen to constrain the rider's motion during an impact. The finite element model was developed using shell elements in the ANSYS 16.0 Composite Pre-Post (ACP) system [12]. Due to the rollover protection system (RPS) being also supported by the fairing, the Analysis of the RPS was performed on vehicle's fairing.

A top load of 2670 N was applied to the top of the roll bar, directed downwards at an angle of 12 degrees from the vertical towards the rear of the vehicle keeping the seat belt attachment points fixed and subject to a reactant force. When the vehicle was subjected to a top load, the load was distributed from the ground to the fairing (Integrated RPS), then to the side rods and the bottom of the frame (both containing the seat belt attachment point). Thereby, protecting body contact from the ground. There was no indication of permanent deformation, fracture, or delamination. The maximum elastic deformation as per the Analysis carried out was 1.0361 cm which was less than the maximum allowable deformation of 5.1 cm, meeting ASME specification. This gave a FOS value of 4.47.

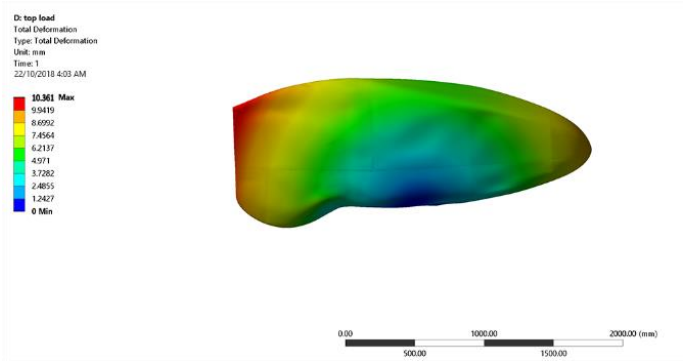

Fig. 7. Total Deformation under action of Top Load on RPS

International Journal of Engineering Research & Technology (IJERT)
ISSN: 2278-0181
Vol. 11 Issue 10, October-2022

A side load of 1330 N was applied horizontally to the side of the roll bar at shoulder height keeping the seat belt attachment points fixed and subject to a reactant force. When the vehicle was subjected to a top load, the load was distributed from the ground to the fairing (Integrated RPS), then to the side rods and the bottom of the frame (both containing the safety harness attachment point). Thereby, protecting body contact from the ground. There was no indication of permanent deformation, fracture, or delamination. The maximum elastic deformation as per the Analysis carried out was 0.79356 cm which was less than the maximum allowable deformation of 3.8 cm, meeting ASME specification. This gave a FOS value of 4.46.

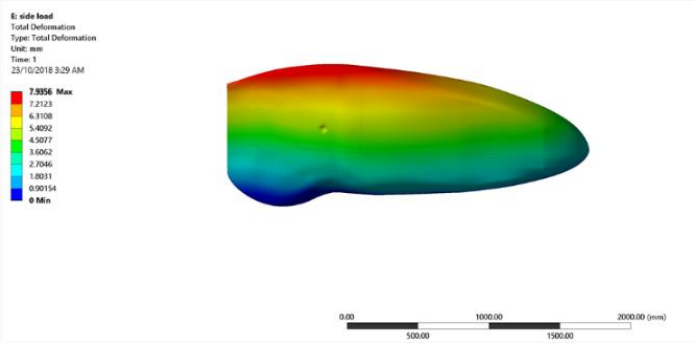

Fig. 8. Total Deformation under action of Side Load on RPS

B. Structural Analysis

Structural Analysis on the frame using ANSYS were carried out measuring the ability of the frame to withstand various stress scenarios which the vehicle may undergo during its normal operation. All the forces were assumed to be below the elastic limit of the material.

Various stresses considered on the bottom bracket include scenarios where the chain experiences large tension force, where there was sudden obstruction leading to considerable friction during the rotation of the pedals, etc. These situations were modelled on the AISI 4130 Chromoly Steel. An automated mesh was developed with an average orthogonal quality of 0.867. A Remote force of 600 N was applied along the Z axis at the (92,0,0) mm from the reference coordinate on the centre of bottom bracket as shown below. The maximum (Von-Mises) stress of 41.089 MPa was observed in the upper section of the Bottom Bracket Coupler showing that there was a FOS of 6.08.

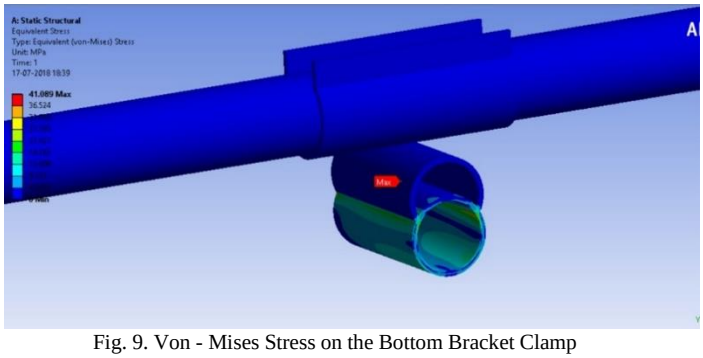

Fig. 9. Von - Mises Stress on the Bottom Bracket Clamp

A significant step to integrate a human-powered vehicle was to ensure that rider comfort was maintained even in rough terrains. The velomobile must be capable of withstanding minor obstacles such as road bumps (with heights up to 9 cm), gravel, sinks and small puddles. An automated mesh was developed with an average orthogonal quality of 0.812. A compressive force of 2802 N along head tube's axis and a bending force of 1201 N at coordinates (-137.62, -408.8, 0) along x-axis considering centre of the head tube as the reference point were applied on the head tube and the deflection produced was analysed in the event of a road bump. The frame displayed a total deformation of 0.144 mm and had a FOS greater than 1. The loading conditions were done according to ASTM F2273-11.

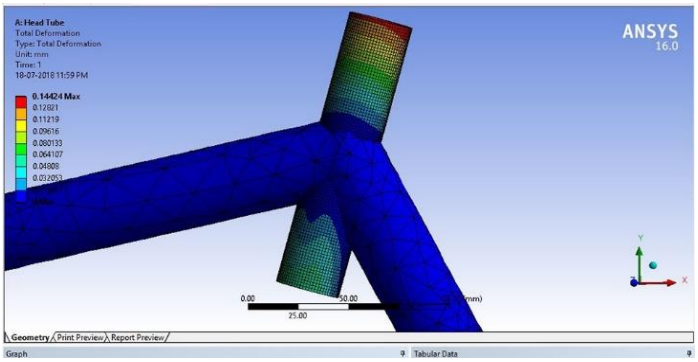

Fig. 10. Total Deformation after Equivalent Stress on the Head Tube

A load of 2500 N was applied towards the front side of the vehicle at the attachment point. The force 2500 N was designed such that the vehicle (weighing ~ 100kgs with rider) travelling at 20 m/s can be stopped within 0.2 seconds. The frame was modelled on ANSYS Space Claim, and the results were analysed on the Static Structural. An automated mesh has been developed with an average orthogonal quality of 0.91. The stress on the seat attachment point was observed to be 149.19 MPa and the total deformation of seat harness 0.9592 mm.

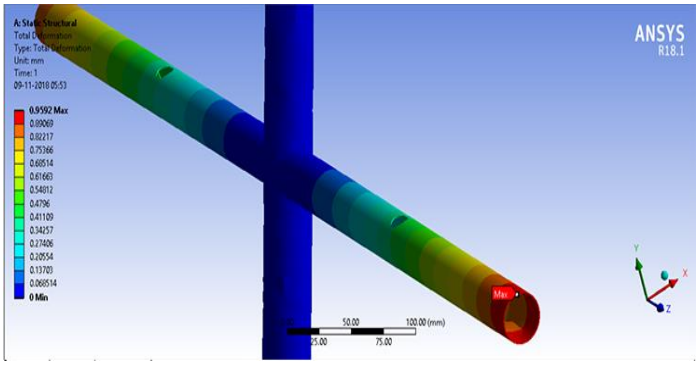

Fig. 11. Total Deformation after Equivalent Stress on the Seat Harness

C. Aerodynamic Analysis

The front wind analysis of the draft fairing was done in Ansys Fluent, and it yielded a drag coefficient of 0.119 (First Iteration) when the maximum speed was assumed to be 20 m/s (72 kmph). The average wind speed was considered as 4.167 m/s (15kmph). For CFD, high emphasis was given on the mesh, every mesh metric was checked so that any inaccuracy.

International Journal of Engineering Research & Technology (IJERT)
ISSN: 2278-0181
Vol. 11 Issue 10, October-2022

RANS based K-Omega Turbulence Model in Steady State, with all y+ wall treatment was chosen as it was not very memory-intensive and yields good convergence even with complex geometries [13]. The model also proved to be stable under high relaxation factors which helped in observing faster convergence without losses in accuracy. After visualization of the flow, an early flow separation was found. To tackle the issue, a guide curve along the rear end of the fairing was incorporated to guide the flow and letting the flow stayed attached for a longer period. The incorporation of the guide curve proved detrimental towards the fairing. The drag coefficient reduced significantly. In the final iteration, the drag coefficient came out to be 0.087 which was much lower than the 1st iteration.

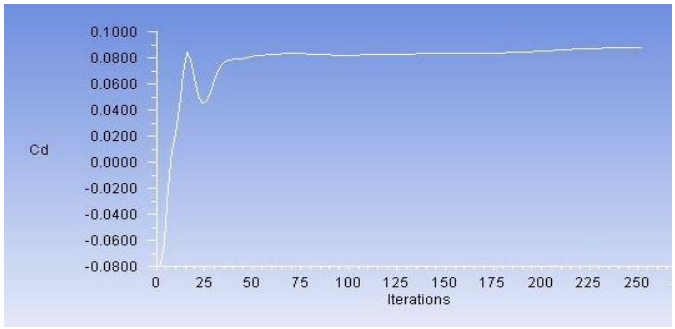

Fig. 12. Cd vs iteration curve

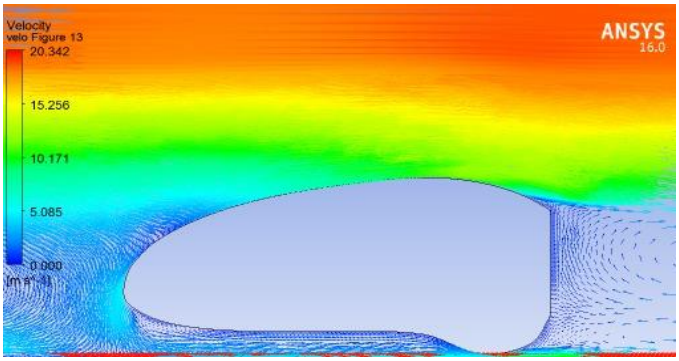

Fig. 13. Velocity contour in a 2.5D Analysis

For observing the large eddy structures in the wake region, the Spalart – Allmaras Detached Eddy Simulation was used with Implicit Unsteady being state of time [14]. Though more computationally intensive it helped understand the effect of cross wind which the vehicle will encounter. Changes were made to ensure that the pressure change across the fairing was significantly lower and the drag force came out to be 9.78 N.

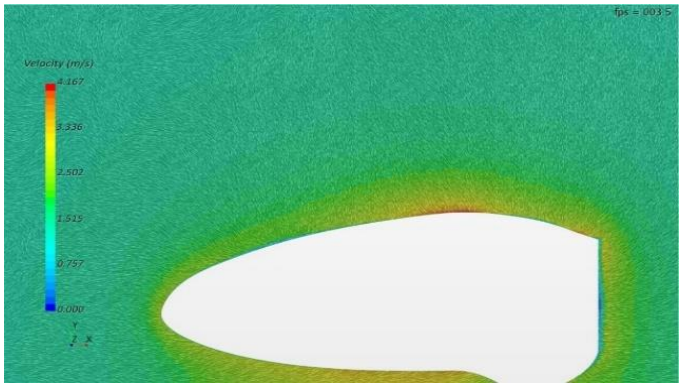

Fig. 14. Velocity Contour around a plane

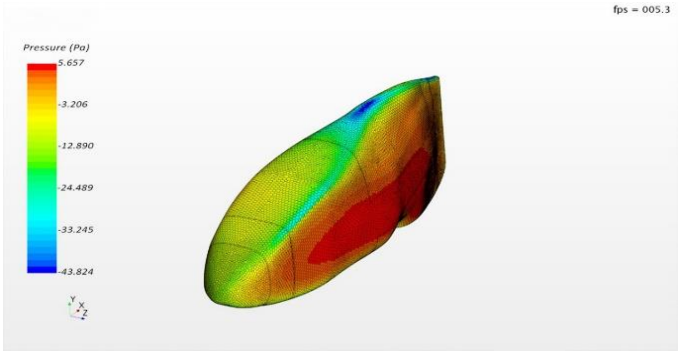

Fig. 15. Pressure distribution w.r.t. atmosphere Analysis

IV. TESTING

A. Heel Strike Testing

Metal prototype model of the preliminary design was made using AISI 1020 Steel to cross check the initial measurements obtained using the jig. Off the shelf (stock) components were used for making the prototype facilitating flexibility for optimization. The mock-up facilitated idler positioning and seat ergonomics, proper steering position and handlebar geometry. To examine the heel and toe curves of the tallest rider for the fairing measurements, the vehicle was aligned with the movement of the rider's leg parallel to the white board and the curve was traced based on the movement of the leg. Both the curves were measured in accordance with the Bottom Bracket of the frame. Both the curves were measured wrt different point of reference (i.e., BB location) depending on the orientation of the board with the vehicle. The heel min and toe max curves were traced and were considered during the fabrication of the fairing for considering the clearance values at the crucial points in the fairing.

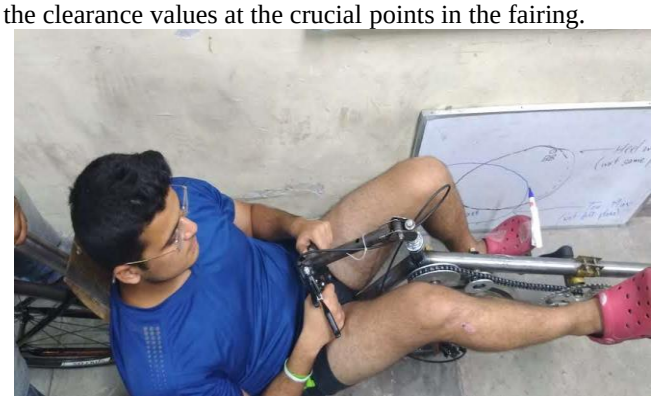

Fig. 16. Measurement of Heel and Toe Curves

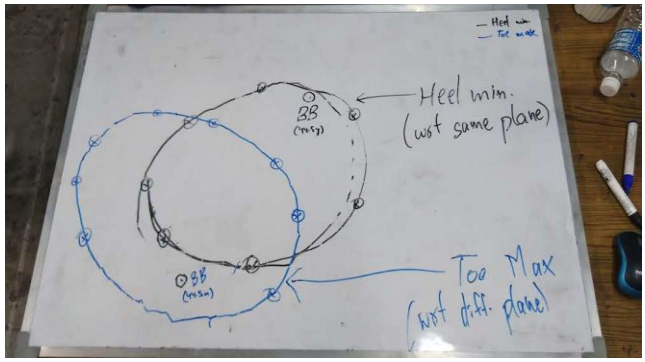

Fig. 17. Toe Max and Heel Min Curves

International Journal of Engineering Research & Technology (IJERT)
ISSN: 2278-0181
Vol. 11 Issue 10, October-2022

B. Fairing Dimensions Testing

To ensure that the fairing can accommodate different riders comfortably, the tallest and shortest riders were made to sit on the bike, and three view photographs were taken. These photos were imported to SolidWorks on the front, top and right planes to give a basic layout of the Vehicle frame with the rider. All the measurements of the crucial points such as pedalling radius, height of rider with helmet, knees and toes, width of shoulders, etc. were plotted on planes whose distances were measured from the centre of front wheel.

The profiles were created, and the fairing was then lofted using these profiles. There was extensive use of Siemens NX 11.0 using its human modelling feature to check clearance at various points in the initial and final verification of the fairing model developed. The fairing was designed according to the vast range of height of riders so that the vehicle can accommodate different riders comfortably.

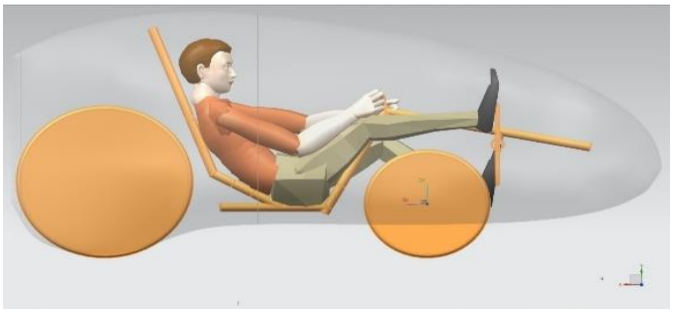

Fig. 18. Human Modelling on NX 11.0

Fig. 19. Frame Dimensions Testing

C. Windshield Material Testing

The windshield area was maximized to increase the field of view. The material was selected based on mold ability and mist formation as the criteria [15]. The molding was done using hot air gun over the glass fiber mold and the material was allowed to acquire the shape of the mold. Acrylic sheets were brittle and could shatter on impact and hence were unsafe to use considering rider's safety. Polycarbonate (Lexan) sheets with thickness 2 mm were selected as ideal material for the windshield.

TABLE 8. OBSERVATIONS OF WINDSHIELD MATERIALS

Material	Thickness	Observation
Polycarbonate (Lexan)	2 mm	Low Mold ability, No Mist
Polycarbonate (Lexan)	4 mm	Poor Mold Ability, Slight Mist
Acrylic (Plexiglass)	2 mm	Good Mold Ability, Slight Mist
Acrylic (Plexiglass)	4 mm	Low Mold Ability, Slight Mist

V. CONCLUSION

The vehicle easily met all the constraints set during the start of the project. Vehicle met the low-speed stability testing (< 5kmph), braking distance testing (25kmph to 0kmph in 6m), turning radius (<8m) requirements. More standard components are recommended instead of customized parts to improve replaceability and decrease cost. Results of the analysis done could also be verified through yarn tuft testing. The project was successful in creating a vehicle in the field of safe and effective Sustainable Transport. Possessing extensive adaptability to challenging operating conditions coupled with enhanced manoeuvrability and robustness makes this innovation a commercially viable alternative.

TABLE 9. COMPARISON OF DESIGN AND ACTUAL VALUES

Metric	Target Value	Estimated Value
Coefficient of Drag	<0.1	0.087
Field of View	225°	In Progress
Turning Radius	<5m	In Progress
Rider Satisfaction	9/10	10/10
Weight	25kg	27kg
Cost	<200,000	1,76,000
Rider Height Range	20cm	18cm
Braking distance from 25kmph speed	< 6m	In Progress
Low Speed Stability	Stable at 5kmph for 30m	In Progress

REFERENCES

[1] M. Ferrari et al., "Development of a hybrid human-electric propulsion system for a velomobile," Eighth International Conference and Exhibition on Ecological Vehicles and Renewable Energies, Monaco, pp. 1-8, 2013.

[2] F. Walle, The velomobile as a vehicle for more sustainable transportation, Royal Institute of Technology, Stockholm, Sweden, 2004.

[3] C. Priyadarsini, B. Khanna, and C. Raviteja, "Design and Analysis of Human Powered Vehicle," International Journal of Management, Technology and Engineering, vol. 9, pp. 3104-3113, January 2019.

[4] A. Olewnik, and K. Lewis, "Limitations of the House of Quality to provide quantitative design information," International Journal of Quality & Reliability Management, vol. 25, pp. 125-146, January 2008.

[5] G. Okudan, and S. Tauhid, "Concept selection methods – a literature review from 1980 to 2008," Int. J. Design Engineering, Vol. 1, pp. 243-277, 2008.

[6] M. Behera, and B. Behera, "Design Failure Modes and Effects Analysis of a Human Powered Recumbent Vehicle," International Journal of Engineering Research & Technology (IJERT), Vol. 5, pp. 27-32, April-2016.

[7] W. Patterson, The Chronicles of the Lords of the Chainring, California Polytechnic State University, 1998.

[8] K. Singh, M. Iyengar, and N. Iyengar, "Design and Analysis of Human Powered Hybrid Vehicle," International Journal of Mechanical Engineering and Technology (IJMET), Vol. 9, pp. 594-605, April 2018.

[9] P. Migliore, "Comparison of NACA 6-Series and 4-Digit Airfoils for Darrieus Wind Turbines," J. Energy, vol. 7, pp. 291-292, August 1983.

[10] R. Selvaraj et al., "Optimisation of swept angles for airfoil NACA 6-series," Int. J. Computer Aided Engineering and Tech., Vol. 9, pp. 229-240, 2017.

[11] R. Jones, Mechanics of Composite Materials, Virginia Polytechnic Institute and State University, 1998.

[12] F. Berg, R. Behling, and M. Helbig, "Rollover crash tests," International Journal of Crashworthiness, vol. 7, pp. 487-498, 2002.

[13] F. Menter, "Influence of Freestream Values on k omega Turbulence Model Predictions." AIAA Journal, Vol. 30, pp. 1657-1659, 2013.

[14] P. Spalart, Detached-Eddy Simulation, Annual Review of Fluid Mechanics, pp. 181-202, January 2009.

[15] Y. Peng et al., "Finite element modeling of crash test behavior for windshield laminated glass," Int. Journal of Impact Engineering, vol. 57, pp. 27-35, 2013.